Comput Geosci (2008) 12:121–132
DOI 10.1007/s10596-007-9064-8

ORIGINAL PAPER

A spectral approach to simulating intrinsic random fields with power and spline generalized covariances

Xavier Emery · Christian Lantuéjoul

Received: 9 August 2007 / Accepted: 20 November 2007 / Published online: 15 January 2008

Abstract This article presents a variant of the spectral turning bands method that allows fast and accurate simulation of intrinsic random fields with power, spline, or logarithmic generalized covariances. The method is applicable in any workspace dimension and is not restricted in the number and configuration of the locations where the random field is simulated; in particular, it does not require these locations to be regularly spaced. On the basis of the central limit and Berry–Esséen theorems, an upper bound is derived for the Kolmogorov distance between the distributions of generalized increments of the simulated random fields and the normal distribution.

Keywords Turning bands method · Spectral simulation · Fractional Brownian sheet · de Wijs process · Generalized increment

1 Introduction

The simulation of random fields is currently used in the geosciences for spatial prediction and uncertainty assessment; see [8] and references therein. The first random field models considered were stationary and Gaussian, i.e., all their finite-dimensional distributions are multinormal and invariant under spatial translation [13, 19, 32, 37]. Application domains include mineral resources evaluation [28], hydrogeology [16], and soil sciences [7], among others. The stationary Gaussian random field model is congenial, insofar as its statistical properties are fully characterized by its mean (constant in space) and its covariance function or, equivalently, its semi-variogram. In practice, the latter is modeled from a sample semi-variogram calculated from the available data. In some circumstances, however, this sample semi-variogram does not have a sill or the data values exhibit a spatial trend (non-constant mean), which makes the stationarity assumption questionable [8].

To overcome this problem, intrinsic random fields of order 0, i.e., random fields with stationary increments, can be considered. A typical example is the fractional Brownian sheet (fractional Brownian motion in 1D), for which the semi-variogram is a power function of the lag distance. In this respect, many simulation algorithms have been proposed in the past decades, based on midpoint displacement approaches [25, 52], continuous and discrete spectral representations [8, 42, 48, 49], wavelet representations [24, 44, 54], dilution of Poisson germs, Poisson hyperplanes and moving averages [8, 35], summation of fractional white noise [53], or simulation of locally equivalent stationary random fields [8, 22, 26]. However, except for simulating a Brownian motion (Wiener–Lévy process), most of these algorithms are approximate or are restricted in the workspace dimension, in the number of locations targeted for simulation, or in their spatial configuration (Table 1).

Fractional Brownian sheets belong to a general family of random fields for which the generalized increments (discrete derivatives from order $k+1$ onward, with $k \in \mathbb{N}$) are stationary. These fields are known as *integrated processes* in time series analysis [3] or *intrinsic random*

X. Emery (✉)
Department of Mining Engineering, University of Chile,
Avenida Tupper 2069,
Santiago 837 0451, Chile
e-mail: xemery@ing.uchile.cl

C. Lantuéjoul
Equipe Géostatistique, Ecole des Mines–ParisTech,
35 Rue Saint-Honoré,
77300 Fontainebleau, France
e-mail: Christian.Lantuejoul@ensmp.fr

Table 1 Properties of current algorithms for simulating fractional Brownian sheets with Hurst coefficient H in $\mathbb{R}^d$

Simulation algorithm	Workspace dimension	Accurate reproduction of semi-variogram?	Normally distributed increments?	Restrictions
Midpoint displacement	1	No[a]	Yes	
Wavelet representations	1	No	No	
Dilution of Poisson germs	1	No[a]	No	
Poisson hyperplanes	d	No[a]	No	
Continuous spectral representations with truncation of low frequencies	d	No	No	
Discrete spectral representations	d	Yes	Yes	Regularly spaced locations
Moving average	1	No[a]	Yes	Idem
Summation of fractional white noise	1	Yes	Yes	Idem
Circulant-embedding approaches	d	Yes	Yes	Idem
Choleski decomposition of covariance matrix	d	Yes	Yes	<5,000 locations
Mixture of locally equivalent random fields with triangular covariances	1	Yes	No	$H \leq 0.5$

[a] These algorithms are accurate when $H=0.5$ and $d=1$, a case that corresponds to the classical Brownian motion (Wiener-Lévy process).

fields of order k in spatial statistics [39]. Their correlation structure is characterized by a generalized covariance function that allows calculating the variance of any generalized increment. As a particular case, for intrinsic random fields of order 0, the generalized covariance is the opposite of the semi-variogram plus an arbitrary constant. An overview of the theory of intrinsic random fields can be found in the paper by Matheron [39] and the textbook by Chilès and Delfiner [8].

Intrinsic random fields of order k are suitable for modeling regionalized variables with trends (*drifts*) that can be represented as polynomial functions of the spatial coordinates. Let us give a few examples of applications in the geosciences:

- In geothermal reservoir modeling, temperature and pressure tend to increase with depth, whereas porosity and permeability tend to decrease. Accordingly, these variables cannot be represented by stationary random fields [9, 50].
- In petroleum reservoir modeling, intrinsic random fields are useful for representing geometrical characteristics (e.g., depth of the top of a dome-shaped structure or anticline trap) or petrophysical properties such as rock porosity [15, 20].
- In groundwater hydrology, the hydraulic gradient is often responsible for a trend in the parameters that characterize an aquifer system (hydraulic head, hydraulic conductivity, transmissivity, total discharge, etc.). The use of intrinsic random fields is all the more satisfactory because these random fields provide the solution of the partial differential equations linking the hydrogeologic parameters [17, 21, 30, 31, 34].
- Other applications include the non-stationary modeling of soil properties [4], mineral grades [11], pollutant concentrations [10], or seafloor depth [5, 12].

This work deals with the simulation of d-dimensional isotropic intrinsic random fields for which the generalized covariance is either a power function of the lag distance, i.e., a function C such that:

$$\forall \boldsymbol{h} \in \mathbb{R}^d, C(\boldsymbol{h}) = (-1)^{k+1} |\boldsymbol{h}|^{\alpha} \tag{1}$$

with $\alpha \in \mathbb{R}_+^*$ and $k \in \mathbb{N}$ such that $2k<\alpha<2k+2$, or a function of the form:

$$\forall \boldsymbol{h} \in \mathbb{R}^d, C(\boldsymbol{h}) = (-1)^{k+1} |\boldsymbol{h}|^{2k} \ln(|\boldsymbol{h}|) \tag{2}$$

with $k \in \mathbb{N}$. The case when $k=1$ and $d=2$ corresponds to the well-known thin plate spline function. For this reason, the function defined in Eq. 2 will be referred to as the spline generalized covariance with index k. The case when $k=0$ is also called logarithmic or "de Wijsian" generalized covariance in the statistical and geostatistical literature [2, 8, 38]. To the best of the authors' knowledge, only the power, spline, and logarithmic generalized covariance models (as well as their linear combinations) have been used in the practice of intrinsic random fields of order k.

The proposed simulation algorithm will be developed so as to fulfill the following requirements:

1. No restriction on the workspace dimension (d).
2. No restriction on the number and spatial configuration of the locations where the random field has to be simulated.
3. Efficiency in terms of time complexity and memory requirement.

4. Accurate reproduction of the generalized covariance (without approximation).
5. Distribution of generalized increments close to normal.

This algorithm is designed in accordance with the principle of the turning bands method [8, 39]. It consists in performing a set of independent one-dimensional simulations and then combining them to produce one d-dimensional simulation. This approach only requires the one-dimensional simulations to possess a power or spline generalized covariance model, as provided by the turning bands operator. Accordingly, the problem of simulating intrinsic random fields in a one-dimensional space is examined first (Section 2); the extension to multi-dimensional spaces using the turning bands method is then considered (Section 3).

2 Simulating random fields with power and spline generalized covariances in $\mathbb{R}$

2.1 Intrinsic random fields with power semi-variograms

This subsection deals with the simulation of a one-dimensional intrinsic random field $Y_{\alpha,1}=\{Y_{\alpha,1}(x):\ x\in\mathbb{R}\}$ that has a power semi-variogram with exponent $\alpha\in]0,2[$:

$$\forall x, x+h\in\mathbb{R}, \frac{1}{2}\mathrm{var}\left\{Y_{\alpha,1}(x)-Y_{\alpha,1}(x+h)\right\}=\ |h|^{\alpha},$$

or, equivalently, a generalized covariance of the form $h\rightarrow -|h|^{\alpha}$ for any real number h. To solve the simulation problem, let us consider a random field of the following form:

$$\forall x\in\mathbb{R}, Y_{\alpha,1}(x)=\theta_{\alpha,1}(R)\ \cos(2\pi R\,x+\phi) \tag{3}$$

where ϕ is a uniform random variable on $[0,2\pi[$ and R is an independent positive random variable with probability density function f_{α}. This expression can be viewed as an extension of traditional spectral approaches to simulating stationary random fields [36, 37, 46, 47], as explained in Appendix. Functions $\theta_{\alpha,1}$ and f_{α} will be chosen so that $Y_{\alpha,1}$ has the required semi-variogram. For any real numbers x and x', one has

$$Y_{\alpha,1}(x)-Y_{\alpha,1}(x')=2\,\theta_{\alpha,1}(R)\ \sin[\pi R(x'-x)]\ \sin[\pi R(x+x')+\phi] \tag{4}$$

As ϕ has a uniform distribution on $[0,2\pi[$ and is independent of R, the increment $Y_{\alpha,1}(x)-Y_{\alpha,1}(x')$ has a zero mean and a variance equal to

$$E\left\{\left[Y_{\alpha,1}(x)-Y_{\alpha,1}(x')\right]^2\right\}=E\left\{2\,\theta^2_{\alpha,1}(R)\ \sin^2[\pi R(x'-x)]\right\}.$$

This variance only depends on $x'-x$; hence, $Y_{\alpha,1}$ has second-order stationary increments. Its semi-variogram at lag h is

$$\begin{aligned}\gamma_{Y_{\alpha,1}}(h)&=E\left\{\theta^2_{\alpha,1}(R)\ \sin^2(\pi R\,h)\right\}\\&=\int_0^{+\infty}\theta^2_{\alpha,1}(r)\,\frac{1-\cos(2\pi r\,h)}{2}\,f_{\alpha}(r)dr\end{aligned} \tag{5}$$

Compare this expression with the spectral representation of the power semi-variogram with exponent α [8]:

$$\forall h\in\mathbb{R}, |h|^{\alpha}=-\frac{2\,\Gamma\left(\frac{1+\alpha}{2}\right)}{\pi^{1/2+\alpha}\Gamma\left(-\frac{\alpha}{2}\right)}\int_0^{+\infty}[1-\cos(2\pi\,r\,h)]\frac{dr}{r^{1+\alpha}}.$$

To have $\gamma_{Y_{\alpha,1}}(h)=|h|^{\alpha}$ for every h, one must find $\theta_{\alpha,1}$ and f_{α} such that

$$\forall r\in\mathbb{R}_+, \frac{1}{2}\theta^2_{\alpha,1}(r)f_{\alpha}(r)=-\frac{2\,\Gamma\left(\frac{1+\alpha}{2}\right)}{\pi^{1/2+\alpha}\Gamma\left(-\frac{\alpha}{2}\right)}\frac{1}{r^{1+\alpha}}. \tag{6}$$

As f_{α} is a probability density function on $\mathbb{R}_+$, the following constraint holds:

$$\int_0^{+\infty}\frac{dr}{\theta^2_{\alpha,1}(r)\,r^{1+\alpha}}<\infty \tag{7}$$

Suppose that there exist two real numbers, β and δ, such that $\theta^2_{\alpha,1}(r)\approx r^{\beta}$ for small r and $\theta^2_{\alpha,1}(r)\approx r^{\delta}$ for large r. To fulfill relation 7, one must have $\beta+\alpha+1<1$ and $\delta+\alpha+1>1$, i.e., $\beta<-\alpha<\delta$. A solution is to define $\theta_{\alpha,1}$ such that

$$\forall r\in\mathbb{R}_+, \theta^2_{\alpha,1}(r)\propto r^{-\alpha/2-1}\,(1+r).$$

Because of Eq. 6, this amounts to putting

$$\forall r\in\mathbb{R}_+, f_{\alpha}(r)\propto\frac{1}{(1+\ r)\,r^{\alpha/2}}.$$

For this function to have a unit integral over $\mathbb{R}_+$, one must take

$$\forall r\in\mathbb{R}_+, f_{\alpha}(r)=\frac{\sin(\pi\,\alpha/2)}{\pi}\,\frac{1}{(1+r)\,r^{\alpha/2}}. \tag{8}$$

One recognizes the probability density function of a beta random variable R of the second kind with parameters $(1-\alpha/2,\ \alpha/2)$. Equivalently, R is the ratio of two independent standard gamma random variables with shape parameters $1-\alpha/2$ and $\alpha/2$, respectively, the simulation of which can easily be achieved by acceptance–rejection algorithms [1, 18, 33]. Note that if α is close to 2, the outcomes of R are likely to be very small: in such a case, the process simulated in Eq. 3 is a low-frequency cosine function and presents long-range memory (or *persistence*), as do fractional Brownian motions with Hurst coefficients close to 1.

If α is close to 0, the outcomes of R are likely to be very large, so that the simulated process is a high-frequency cosine function and presents anti-persistence.

According to Eqs. 6 and 8, function $\theta_{\alpha,1}$ is defined by

$$\forall r \in \mathbb{R}_+, \theta_{\alpha,1}(r) = \sqrt{\frac{4\,\Gamma(\alpha+1)\,(1+r)}{(2\pi)^{\alpha} r^{\alpha/2+1}}}. \tag{9}$$

2.2 Intrinsic random fields with power generalized covariances

In this study, we consider the general problem of simulating an intrinsic random field in $\mathbb{R}$ with the generalized covariance $h \to (-1)^{k+1}|h|^{\alpha}$, where α is a positive real number and k is the integer part of $\alpha/2$. For $\alpha<2$, this boils down to simulating an intrinsic random field with a power semi-variogram of exponent α, which has been solved in the previous subsection. In what follows, only the case $\alpha \geq 2$ is examined.

Let k be a positive integer, α a real number in $]2k,2k+2[$ and ϕ a uniform random variable on $[0,2\pi[$. Consider a random field $Y_{\alpha,1}$ such that

$$\forall x \in \mathbb{R}, Y_{\alpha,1}(x) = \theta_{\alpha,1}(R)\,\cos(2\pi R\,x + \phi), \tag{10}$$

for a random variable R independent of ϕ and a function $\theta_{\alpha,1}$ to determine. Its derivative of order k is defined by

$$\forall x \in \mathbb{R}, Y^{(k)}_{\alpha,1}(x) = \theta_{\alpha,1}(R)(2\pi R)^k \cos(2\pi R\,x + \phi'), \tag{11}$$

where $\phi' = \phi + k\pi/2 (\mathrm{mod}\, 2\pi)$ is a uniform random variable on $[0,2\pi[$. Assume that $Y_{\alpha,1}$ has the requested power generalized covariance $h \to (-1)^{k+1}|h|^{\alpha}$. Then, $Y^{(k)}_{\alpha}$ has the generalized covariance [8]:

$$\forall h \in \mathbb{R}^*, h \to (-1)^k \frac{d^{2k}}{dh^{2k}}\left\{(-1)^{k+1}\,|h|^{\alpha}\right\},$$

that is

$$\forall h \in \mathbb{R}^*, h \to -\frac{\Gamma(\alpha+1)}{\Gamma(\alpha-2k+1)}|h|^{\alpha-2k}.$$

Because the exponent of this power covariance $(\alpha-2k)$ is less than 2, one can choose for $Y^{(k)}_{\alpha,1}$ a random field proportional to that introduced in Eq. 3:

$$\forall x \in \mathbb{R}, Y^{(k)}_{\alpha,1}(x) = \sqrt{\frac{\Gamma(\alpha+1)}{\Gamma(\alpha-2k+1)}} Y_{\alpha-2k,1}(x). \tag{12}$$

By identifying Eqs. 11 and 12, one finds that R is a beta random variable with density $f_{\alpha-2k}$, as defined in Eq. 8, whereas $\theta_{\alpha,1}$ is such that:

$$\begin{aligned}\forall r \in \mathbb{R}_+, \theta_{\alpha,1}(r) &= \frac{\theta_{\alpha-2k,1}(r)}{(2\pi r)^k}\sqrt{\frac{\Gamma(\alpha+1)}{\Gamma(\alpha-2k+1)}} \\ &= \sqrt{\frac{4\,\Gamma(\alpha+1)\,(1+r)}{(2\pi)^{\alpha} r^{\alpha/2+k+1}}}\end{aligned}$$

2.2.1 Comments

1. Numerical problems may occur if the outcome of R is close to 0, as $\theta_{\alpha,1}(r)$ behaves like $r^{-(\alpha/2+k+1)/2}$ for small r values. A solution is to replace the cosine function in Eq. 10 by its Lagrange remainder at order k by putting

$$Y_{\alpha,1}(x) = \theta_{\alpha,1}(R)\left\{\cos(2\pi R\,x+\phi) - \sum_{p=0}^{k}\frac{(2\pi R\,x)^p}{p\,!}\cos\left(\phi + p\frac{\pi}{2}\right)\right\}. \tag{13}$$

   The generalized covariance of $Y_{\alpha,1}$ is unchanged, as an intrinsic random field of order k is defined up to a polynomial of degree k: Two random fields that differ from a polynomial of degree k or less are indistinguishable from the viewpoint of generalized increments of order k [8].

2. The probability density function $f_{\alpha-2k}$ is undefined if α is an even integer, say $\alpha=2k$ with $k \in \mathbb{N}^*$, so that Eq. 10 cannot be used in this case. An intrinsic random field with the power covariance $h \to (-1)^k|h|^{2k}$ and with normal generalized increments can, however, be obtained by putting

$$\begin{aligned}\forall x \in \mathbb{R}, Y_{2k,1}(x) &= A\,\frac{\sqrt{\Gamma(2k+1)}}{\Gamma(k+1)}\,x^k \\ &= A\sqrt{\frac{\Gamma\left(\frac{1}{2}+k\right)}{\Gamma\left(\frac{1}{2}\right)\Gamma(k+1)}}\,(2x)^k\end{aligned} \tag{14}$$

   where A is a standard normal random variable. The proof for Eq. 14 is similar to that made in Eqs. 10 to 12 and consists in checking that the generalized covariance of the kth derivative of $Y_{2k,1}$ is

$$h \to \Gamma(2k+1) = (-1)^k \frac{d^{2k}}{dh^{2k}}\left\{(-1)^{k+1}|h|^{2k}\right\}.$$

2.3 Intrinsic random fields with spline generalized covariances

Other options are possible to choose functions $\theta_{\alpha,1}$ and f_α that fulfill the condition given in Eq. 7, for instance,

$$\forall r \in \mathbb{R}_+, \forall \alpha \in]0,2[, \begin{cases} \theta'_{\alpha,1}(r) = \sqrt{-\frac{4\pi\,\Gamma\left(\frac{1+\alpha}{2}\right)(1+r)}{\Gamma\left(-\frac{\alpha}{2}\right)(\pi r)^{\alpha+1/2}}} \\ f'_\alpha(r) = \frac{1}{\pi}\frac{1}{(1+r)\sqrt{r}} \end{cases} \quad (15)$$

As in the previous subsection, this result can be used for simulating an intrinsic random field with the power generalized covariance (1) in $\mathbb{R}$. Let α be a positive real number (not necessarily less than 2) different from an even integer and k be the integer part of $\alpha/2$. All calculations done, one finds a random field of the following form:

$$\forall x \in \mathbb{R}, Y'_{\alpha,1}(x) = \theta'_{\alpha,1}(R')\,\cos(2\pi R' x + \phi), \quad (16)$$

where ϕ is a uniform random variable on $[0,2\pi[$, R' is an independent random variable with probability density function f'_α, and $\theta'_{\alpha,1}$ is defined by:

$$\theta'_{\alpha,1}(r) = \sqrt{-\frac{\pi^{1/2-\alpha}\,\Gamma(\alpha+1)\Gamma\left(\frac{1+\alpha}{2}-k\right)(1+r)}{2^{2k-2}\Gamma(\alpha-2k+1)\,\Gamma\left(k-\frac{\alpha}{2}\right)r^{\alpha+1/2}}}$$

An interesting feature of this approach is that the probability density function of R' defined in Eq. 15 does no longer depend on the value of α: R' is a beta random variable of the second kind with parameters 1/2 and 1/2, i.e. the ratio of two independent standard gamma random variables with shape parameter 1/2. This will be useful for generalizing the proposed method to the simulation of random fields with spline generalized covariances.

Let us consider a family $\{Y'_{2k+\varepsilon,1} : \varepsilon \in \mathbb{R}_+^*\}$ of intrinsic random fields of order k defined as in Eq. 16 with the same pair of random variables (R',ϕ). Define a new family of random fields $\{S_{2k+\varepsilon,1} : \varepsilon \in \mathbb{R}_+^*\}$ in the following fashion:

$$\forall \varepsilon \in \mathbb{R}_+^*, \forall x \in \mathbb{R}, S_{2k+\varepsilon,1}(x) = \frac{1}{\sqrt{\varepsilon}} Y'_{2k+\varepsilon,1}(x). \quad (17)$$

The generalized covariance of $S_{2k+\varepsilon,1}$ (denoted by $C_{S_{2k+\varepsilon,1}}$) is that of $Y'_{2k+\varepsilon,1}$ divided by ε:

$$\forall h \in \mathbb{R}, C_{S_{2k+\varepsilon,1}}(h) = \frac{(-1)^{k+1}|h|^{2k+\varepsilon}}{\varepsilon}.$$

As the generalized covariance of an intrinsic random field of order k is defined up to an even polynomial of degree $2k$ [8], one can also write

$$\forall h \in \mathbb{R}, C_{S_{2k+\varepsilon,1}}(h) \equiv (-1)^{k+1}\left\{\frac{|h|^{2k+\varepsilon}-|h|^{2k}}{\varepsilon}\right\}.$$

If ε tends to zero, it is seen that $\{C_{S_{2k+\varepsilon,1}} : \varepsilon \in \mathbb{R}_+^*\}$ tends to a spline generalized covariance with index k

$$\forall h \in \mathbb{R}^*, C_{S_{2k+\varepsilon,1}}(h) \xrightarrow[\varepsilon\to 0]{} C_{S_{2k,1}}(h) = (-1)^{k+1}|h|^{2k}\,\ln(|h|).$$

Therefore, an intrinsic random field with the generalized covariance (2) in $\mathbb{R}$ is obtained by putting:

$$\forall x \in \mathbb{R}, S_{2k,1}(x) = \xi_{2k,1}(R')\,\cos(2\pi R' x + \phi), \quad (18)$$

with

$$\forall r \in \mathbb{R}_+, \xi_{2k,1}(r) = \lim_{\varepsilon\to 0}\frac{\theta'_{2k+\varepsilon,1}(r)}{\sqrt{\varepsilon}} = \sqrt{\frac{\Gamma(2k+1)(1+r)}{(2\pi)^{2k-1}r^{2k+1/2}}} \quad (19)$$

2.4 Random measures with logarithmic generalized covariances

The previous statements from Eqs. 17 to 19 are valid for $k=0$, which corresponds to the logarithmic generalized covariance. Strictly speaking, this covariance is not associated with an intrinsic random field, rather with a random measure, as it is unbounded and cannot be extended at $h=0$. However, the regularization of such a random measure onto a non-point support corresponds to an intrinsic random field [38]. For instance, the regularized random field over an interval of length $2a$ is

$$\overline{S}_{0,1}(x) = \frac{1}{2a}\int_{-a}^{a}\xi_{0,1}(R')\,\cos[2\pi R'(x+u)+\phi]\,du = \sqrt{\frac{1+R'}{2\pi a R'^{5/2}}}\sin(2\pi a R')\cos(2\pi R' x+\phi)$$

3 Simulating random fields with isotropic power and spline generalized covariances in $\mathbb{R}^d$: Turning bands method

3.1 Intrinsic random fields with power generalized covariances

Simulating an intrinsic random field with the isotropic power generalized covariance (1) in $\mathbb{R}^d$ ($d\geq 1$) is done by recourse to the turning bands method by putting [8, 39]

$$\forall \boldsymbol{x} \in \mathbb{R}^d, Y_{\alpha,d}(\boldsymbol{x}) = \frac{1}{\sqrt{A_{\alpha,d}}} Y_{\alpha,1}(<\boldsymbol{x},\boldsymbol{U}>), \quad (20)$$

where $\boldsymbol{U}$ is a random vector uniformly distributed on the unit hypersphere of $\mathbb{R}^d$, $<\,,\,>$ is the standard inner product in $\mathbb{R}^d$, and $A_{\alpha,d}$ is defined by:

$$A_{\alpha,d} = \frac{\Gamma\left(\frac{d}{2}\right)\,\Gamma\left(\frac{1+\alpha}{2}\right)}{\Gamma\left(\frac{1}{2}\right)\,\Gamma\left(\frac{d+\alpha}{2}\right)}.$$

Let us consider the case when α is a positive real number different from an even integer and define k as the integer part of $\alpha/2$. Formula 20 amounts to putting

$$\forall \boldsymbol{x} \in \mathbb{R}^d, Y_{\alpha,d}(\boldsymbol{x}) = \theta_{\alpha,d}(R)\ \cos\big(2\pi R\ <\boldsymbol{x},\boldsymbol{U}>+\phi\big), \quad (21)$$

where ϕ is a uniform random variable on $[0,2\pi[$, R is an independent beta random variable with the density $f_{\alpha-2k}$ defined in Eq. 8, and $\theta_{\alpha,d}$ is given by

$$\forall r \in \mathbb{R}_+, \theta_{\alpha,d}(r) = \frac{\theta_{\alpha,1}(r)}{\sqrt{A_{\alpha,d}}} = \sqrt{\frac{4\,\Gamma\left(\frac{\alpha}{2}+1\right)\Gamma\left(\frac{d+\alpha}{2}\right)(1+r)}{\Gamma\left(\frac{d}{2}\right)\pi^{\alpha} r^{\alpha/2+k+1}}}$$

Again, to avoid numerical problems when the outcome of R is very small, one can trade the cosine function in Eq. 21 for its Lagrange remainder at order k; see Eq. 13.

When α is an even integer ($\alpha=2k$ with $k\in\mathbb{N}^*$), Eq. 20 becomes

$$\forall \boldsymbol{x} \in \mathbb{R}^d, Y_{2k,d}(\boldsymbol{x}) = A\sqrt{\frac{\Gamma\left(\frac{d}{2}+k\right)}{\Gamma\left(\frac{d}{2}\right)\Gamma(k+1)}}\ <2\boldsymbol{x},\boldsymbol{U}>^{\mathbf{k}}, \quad (22)$$

where A is a standard normal random variable.

The turning bands method for simulating intrinsic random fields with power generalized covariances has already been proposed by several authors [20, 41, 43, 53]. However, these proposals use algorithms that perform the simulation only at regularly spaced locations along the line spanned by vector $\boldsymbol{U}$. The simulated values must, therefore, be migrated to the projection of the locations of interest in $\mathbb{R}^d$ onto the line [37, 43]. Such a migration yields a bias in the reproduction of the generalized covariance model and causes difficulties in memory management if the discretization mesh (band width) is small in comparison with the size of the interval to be simulated on the line [22]. In the present work, the line simulation process uses functions that are defined continuously (Eqs. 21 and 22) and can be calculated at any set of locations, not necessarily at regularly spaced locations. There is no need for discretization and migration, so that the generalized covariance model is reproduced accurately.

3.2 Intrinsic random fields with spline generalized covariances

The results given in Section 2.3 can also be extended to simulating by turning bands an intrinsic random field with the isotropic spline generalized covariance (2) in $\mathbb{R}^d$. All calculations done, one finds a random field of the following form:

$$\forall k \in \mathbb{N}, S_{2k,d}(\boldsymbol{x}) = \xi_{2k,d}(R')\ \cos\left(2\pi R' <\boldsymbol{x},\boldsymbol{U}>+\phi\right), \quad (23)$$

with R' and ϕ defined as in Eq. 16 and

$$\forall r \in \mathbb{R}_+, \xi_{2k,d}(r) = \sqrt{\frac{2\,\Gamma\left(\frac{d}{2}+k\right)\Gamma(k+1)(1+r)}{\pi^{2k-1}\,\Gamma\left(\frac{d}{2}\right)\,r^{2k+1/2}}}.$$

The case when $k=0$ corresponds to a random measure with logarithmic (de Wijsian) generalized covariance. Let $\varpi_d(a) = \frac{a^d\pi^{d/2}}{\Gamma\left(\frac{d}{2}+1\right)}$ denote the volume of a ball of $\mathbb{R}^d$ with radius a. By regularizing the random measure over such a ball, one obtains

$$\begin{aligned}\overline{S}_{0,d}(\boldsymbol{x}) &= \tfrac{1}{\varpi_d(a)}\int_{-a}^{a}\varpi_{d-1}\left(\sqrt{a^2-u^2}\right)\xi_{0,d}(R')\eta(u)du \\ &= \Gamma\left(\tfrac{d}{2}+1\right)\sqrt{\tfrac{2\,(1+R')}{a^d\pi^{d-1}R'^{d+1/2}}}\,J_{d/2}(2\pi a\,R')\eta(0)\end{aligned} \quad (24)$$

where $\eta(u) = \cos[2\pi R'(<\boldsymbol{x},\boldsymbol{U}>+u)+\phi]$ and $J_{d/2}$ is the Bessel function of the first kind with index $d/2$. The second identity in Eq. 24 has been obtained by using the Poisson integral representation [27].

3.3 Towards normal generalized increments

Up to now, the algorithm specified by Eqs. 21 and 23 fulfills all the requirements stated in Section 1, except the last one (the generalized increments are not normally distributed). To overcome this situation, the usual practice is to define a normalized sum of the form

$$\forall \alpha \in \mathbb{R}_+^*, Y_{\alpha,d,N}(\boldsymbol{x}) = \frac{1}{\sqrt{N\,A_{\alpha,d}}}\sum_{i=1}^{N} Y_{\alpha,1}^{(i)}(<\boldsymbol{x},\boldsymbol{U}_i>), \quad (25)$$

or

$$\forall k \in \mathbb{N}, S_{2k,d,N}(\boldsymbol{x}) = \frac{1}{\sqrt{N\,A_{2k,d}}}\sum_{i=1}^{N} S_{2k,1}^{(i)}(<\boldsymbol{x},\boldsymbol{U}_i>) \quad (26)$$

where $\{\boldsymbol{U}_i,\ i=1\ldots N\}$, $\{Y_{\alpha,1}^{(i)}, i=1\ldots N\}$ and $\{S_{2k,1}^{(i)}, i=1\ldots N\}$ are independent random vectors and random fields defined as in Eqs. 20 or 23. Under these conditions, the generalized covariance of $Y_{\alpha,d,N}$ (respectively, of $S_{2k,d,N}$) is the same as that of $Y_{\alpha,d,1}$ (respectively, of $S_{2k,d,1}$) [8]. Besides, because of the central limit theorem, the generalized increments of $Y_{\alpha,d,N}$ and $S_{2k,d,N}$ tend to be normally distributed as N becomes infinitely large.

As an illustration of the method, Figs. 1 and 2 present grayscale representations of isotropic intrinsic random fields on a square grid of $\mathbb{R}^2$, obtained by using $N=50{,}000$ basic random fields. The representations displayed

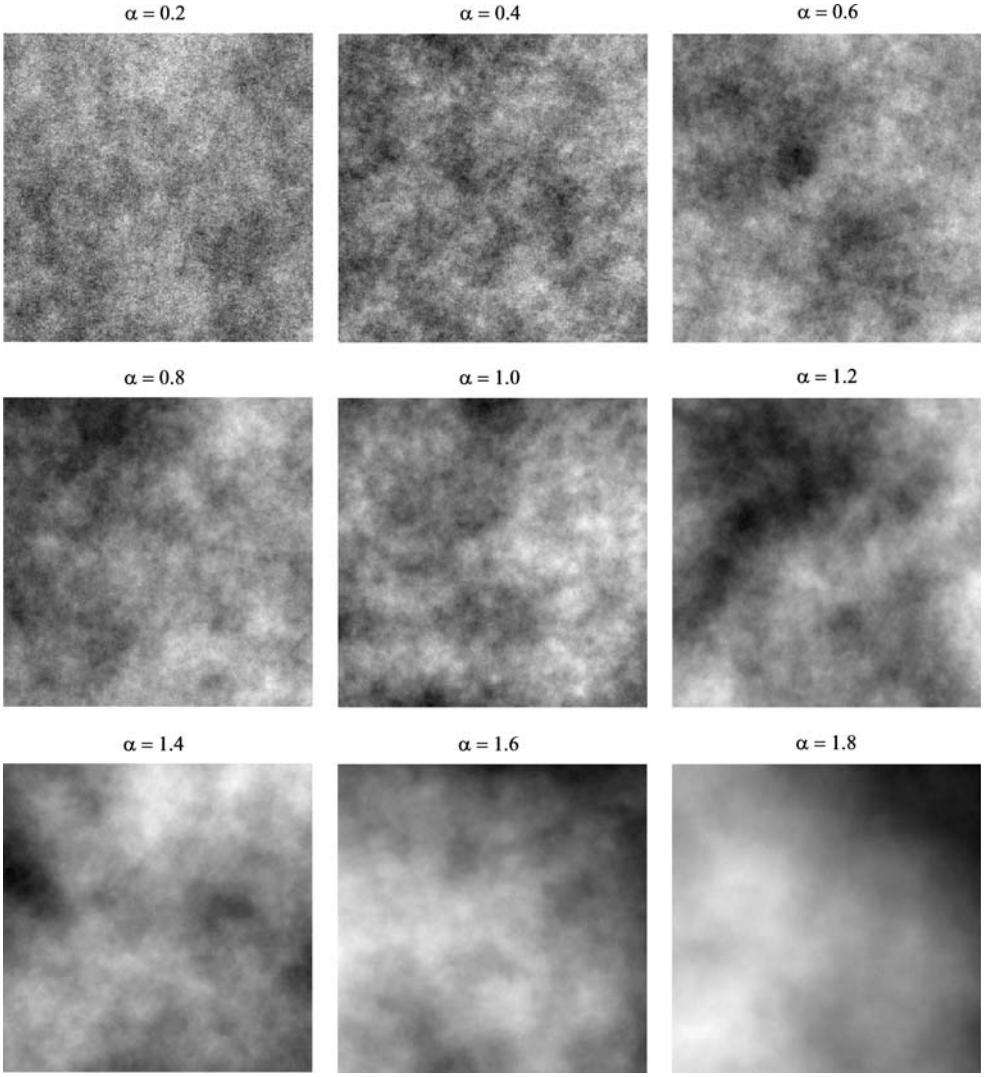

Fig. 1 Realizations of two-dimensional intrinsic random fields with isotropic power semi-variograms of exponent α. These realizations have been drawn on a regular grid with 200×200 nodes by using the turning bands method with N=50,000 independent random fields defined as in Eq. 21. From *left to right* and *top to bottom*, α=0.2, 0.4, 0.6, 0.8, 1.0, 1.2, 1.4, 1.6, and 1.8

in Fig. 1 are realizations of random fields with power semi-variograms that approximate the fractional Brownian sheet in $\mathbb{R}^2$. The representations of Fig. 2 correspond to a random measure with a logarithmic generalized covariance regularized onto balls with radius a equal to 0.1 and 1 times the grid spacing, respectively.

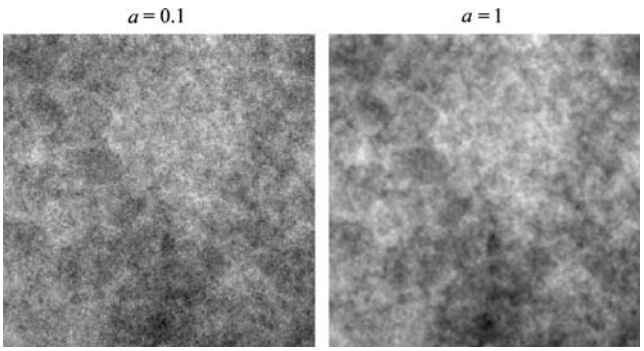

Fig. 2 Realizations of regularized random measures with isotropic logarithmic (de Wijsian) generalized covariances. These realizations have been drawn on a regular grid with 200×200 nodes by using the turning bands method with N=50,000 independent random fields defined as in Eq. 24, with a regularization radius equal to 0.1 (*left*) and 1 (*right*) times the grid spacing

One is also interested in knowing the rate of convergence of the generalized increment finite-dimensional distributions to normal distributions when N increases. As an example, let us consider the simulation of an intrinsic random field with a power semi-variogram ($0<\alpha<2$) in $\mathbb{R}$ (Section 2.1). The Berry–Esséen inequality [23] provides an upper bound for the Kolmogorov distance between the distribution of a standardized increment and the asymptotical normal distribution:

$$\sup_{y\in\mathbb{R}}\left|P\left\{\frac{Y_{\alpha,1,N}(x+h)-Y_{\alpha,1,N}(x)}{\sqrt{2|h|^{\alpha}}}<y\right\}-G(y)\right| \leq \frac{\kappa}{\sqrt{N}}\,\mu_3(\alpha,h), \tag{27}$$

where G is the standard normal cumulative distribution function, κ is a constant less than 0.7655 [45], and $\mu_3(\alpha,h)$

is the third order absolute moment of the standardized increment of $Y_{\alpha,1,1}$:

$$\mu_3(\alpha,h) = E\left\{\left|\frac{Y_{\alpha,1,1}(x+h) - Y_{\alpha,1,1}(x)}{\sqrt{2\,|h|^{\alpha}}}\right|^3\right\}.$$

By using Eq. 4, this moment can be expressed as:

$$\mu_3(\alpha,h) = \frac{8}{(2\,|h|^{\alpha})^{3/2}}\,\frac{4}{3\pi}E\left\{\theta^3_{\alpha,1}(R)\,|\sin(\pi R h)|^3\right\}.$$

From Cauchy–Schwarz inequality and Eqs. 5, 8, and 9, it comes

$$E\left\{\theta^3_{\alpha,1}(R)\;|\sin(\pi R h)|^3\right\} \le |h|^{\alpha/2}\,\frac{4\,\Gamma(\alpha+1)}{(2\pi)^{\alpha}} \times\sqrt{\frac{\sin(\pi\alpha/2)}{\pi}\int_0^{+\infty}\frac{1+r}{r^{3\alpha/2+2}}\,\sin^4(\pi r h)\,dr}.$$

The integral can be expressed by using the following identity, valid for $a\in]0,4[-\{1,2,3\}$:

$$\int_0^{+\infty}\frac{\sin^4(u)\,du}{u^{a+1}} = \frac{\pi\,2^{a-2}(1-2^{a-2})}{\Gamma(1+a)\,\sin\left(\frac{a\pi}{2}\right)}.$$

Suppose that α is different from 2/3 and 4/3. It ensues:

$$\mu_3(\alpha,h) \le \frac{2^{9/2-\alpha/4}\Gamma(\alpha+1)}{3\pi^{1+\alpha/4}\,|h|^{\alpha/4}} \times\sqrt{\frac{\sin\left(\frac{\pi\alpha}{2}\right)}{\Gamma\left(1+\frac{3\alpha}{2}\right)}\left\{h\,\frac{2\pi\,(1-2^{3\alpha/2-1})}{\left(1+\frac{3\alpha}{2}\right)\,\cos\left(\frac{3\alpha\pi}{4}\right)} + \frac{1-2^{3\alpha/2-2}}{\sin\left(\frac{3\alpha\pi}{4}\right)}\right\}}. \tag{28}$$

The upper bound can be extended for α=2/3 and α=4/3 in the following fashion:

$$\begin{cases}\mu_3\left(\frac{2}{3},h\right) \le \frac{1}{|h|^{1/6}}\,\frac{2^{10/3}\,\Gamma\left(\frac{5}{3}\right)}{3^{3/4}\,\pi^{7/6}}\,\sqrt{4\,|h|\,\ln(2)+1}\\ \mu_3\left(\frac{4}{3},h\right) \le \frac{1}{|h|^{1/3}}\,\frac{2^{11/3}\Gamma\left(\frac{7}{3}\right)}{3^{5/4}\,\pi^{11/6}}\,\sqrt{\pi^2|h|+3\,\ln(2)}\end{cases} \tag{29}$$

Figure 3 presents the results corresponding to four lag distances: h=1, 0.5, 0.1, and 0.05. It is seen that $\mu_3(\alpha,h)$ is always less than 2.3 for all these lags. Accordingly, by using N=50,000 basic random fields, Eq. 27 ensures that the Kolmogorov distance between the distribution of standardized increments and the standard normal distribution will be less than 0.008.

Several comments are worth being made:

1. Inequalities 28 and 29 indicate that $\mu_3(\alpha,h)$ is likely to be large when $|h|$ tends to 0 or to infinity, thus, do not provide any information about the rate of convergence to normality. This suggests that the distributions of short-scale and large-scale increments may depart from normality much more than those of medium-scale increments. Indeed, it is difficult to reproduce the short-scale and large-scale behaviors of fractional Brownian motions by summing cosine functions, as these are infinitely differentiable and periodic (in particular, a large number of low-frequency cosine functions must be used before periodicities become indiscernible at the scale of the domain on which simulation is performed).
2. The Berry–Esséen inequality is conservative and may be loose for the case of interest: convergence to normality may be faster than that indicated in Eq. 27.
3. Convergence to normality may also be improved by using in Eq. 25 a set of vectors $\{\boldsymbol{U}_i, i=1\ldots N\}$ regularly or quasi-regularly distributed over the unit hypersphere of $\mathbb{R}^d$, instead of independent uniform vectors. For instance, vectors regularly distributed on the unit circle of $\mathbb{R}^2$ can be used for any value of N. In higher dimensional spaces, the number of regularly distributed vectors on the unit hypersphere is bounded (e.g., $N\le$15 in $\mathbb{R}^3$). To overcome this restriction, one can use equidistributed sequences with low discrepancy [32], the distribution of which is more homogeneous over the unit sphere than that of independent uniform vectors.
4. Regarding the simulation of intrinsic random fields with spline generalized covariances, the third-order absolute moments of the generalized increments of $S_{2k,d}$ are not always finite. Accordingly, when using a normalized sum of the form 26, the upper bound of the Berry–Esséen inequality may not exist, and the rate of convergence to normality remains unknown.

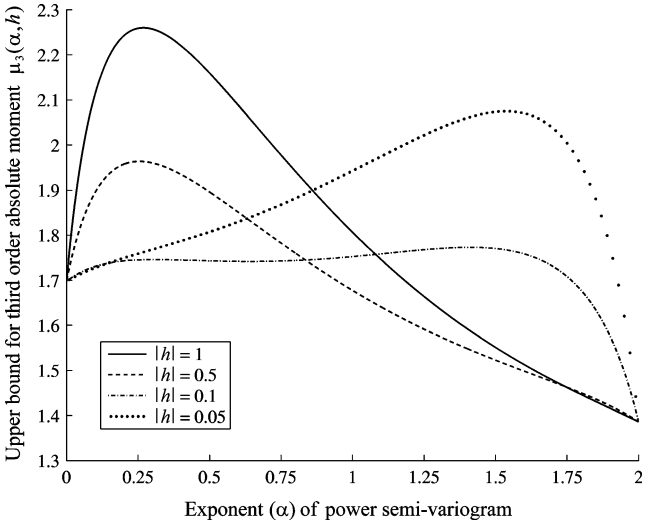

Fig. 3 Theoretical upper bounds for the third order absolute moment $\mu_3(\alpha,h)$ for $|h|$=1, 0.5, 0.1, and 0.05. This moment refers to the standardized increment of a one-dimensional intrinsic random field $Y_{\alpha,1,1}$ with semi-variogram $h \to |h|^{\alpha}$

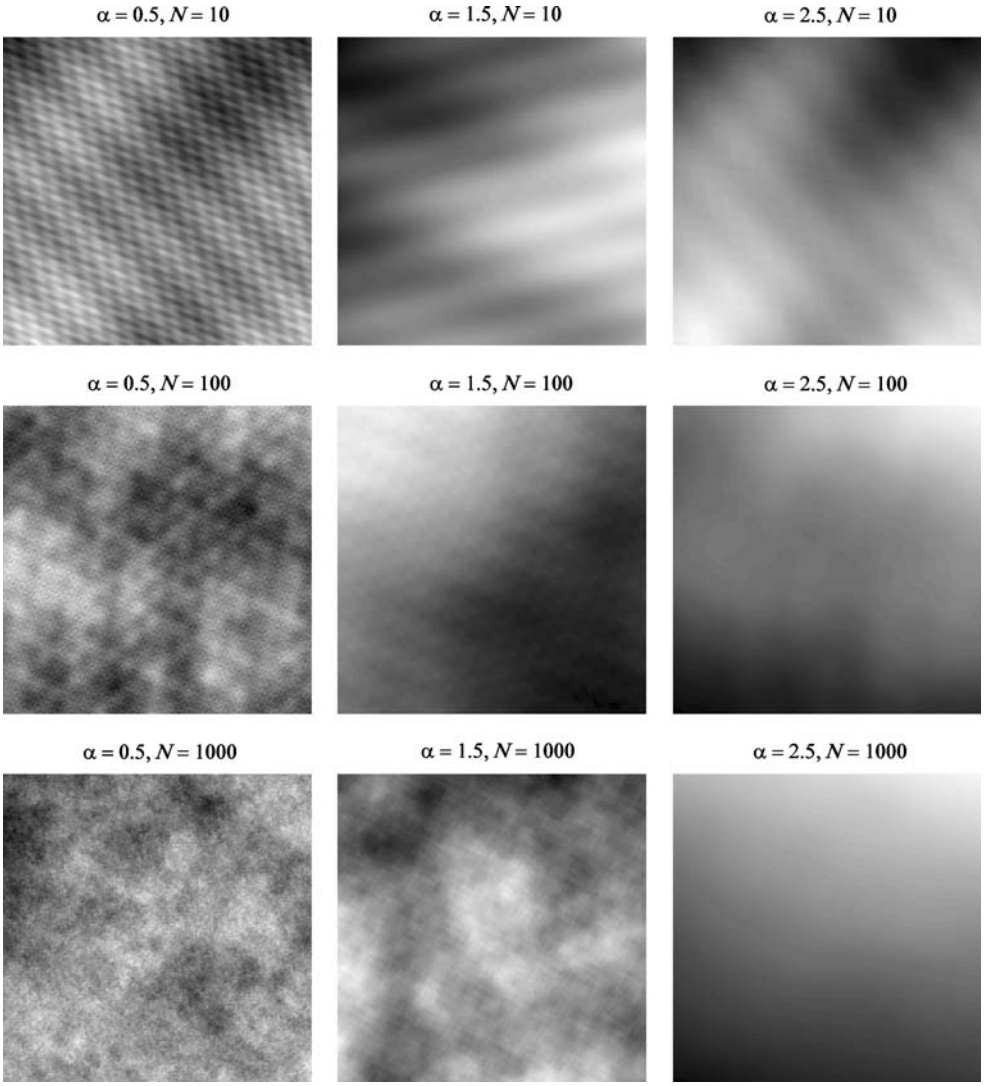

Fig. 4 Realizations of intrinsic random fields with isotropic power generalized covariances of exponent α. These realizations have been drawn on a regular grid of $\mathbb{R}^3$ by using the turning bands method with varying values for N (only a planar cross-section is displayed)

5. Other criteria can be considered for assessing whether the distributions of generalized increments are close to normal or not. In [32, 33], it is proposed to compare the fourth-order moments of increments with those of a normal distribution, and it is shown that this criterion is less severe than the Kolmogorov distance criterion.
6. *Banding effect*. From Eq. 25, it is seen that $Y^{(i)}_{\alpha,1}$ does not contribute to the variability of $Y_{\alpha,d,N}$ in the hyperplane orthogonal to vector $\boldsymbol{U}_i$, which tends to produce linelike patterns ("banding" or "stripping" effect) when mapping the realizations of $Y_{\alpha,d,N}$ [37, 51]. To attenuate these patterns, it is advisable to use several hundreds or thousands of basic random fields [8, 22, 51]. An example is given in Fig. 4, which maps realizations of $Y_{\alpha,3,N}$ for several values of α and N: Banding is manifest with N=10 and still appears with N=100 and α=0.5 or 1.5, but it becomes barely visible with N=1,000 in all the cases. From several thousands of basic random fields onward, banding is imperceptible (as seen in Figs. 1 and 2, which have been obtained with N=50,000). Accordingly, choosing a large number for N not only ensures that the generalized increments are normally distributed but also eliminates the linelike patterns in the simulated maps. The computational cost is not really a problem because of the very simple expression of the basic random fields (Eqs. 21 to 23).

4 Concluding remarks

The algorithm presented in this work is an extension of the so-called *spectral turning bands* method [32, 36, 37] for simulating multi-dimensional intrinsic random fields instead of stationary random fields. It is fast and accurate in the sense that the target generalized covariance (power, spline, or logarithmic model) is reproduced exactly, irrespective of the number of basic random fields considered in the turning bands process.

Because it uses functions defined continuously (cosine functions), the proposed algorithm allows performing the simulation at any set of locations in $\mathbb{R}^d$, which cannot be done with the moving average, discrete spectral, and circulant-embedding approaches. Let us give a few examples in which this feature is useful.

1. Domain shape. Suppose that the random field has to be simulated on a bounded domain $D \subset \mathbb{R}^d$. Using algorithms that only perform the simulation on regular grids may not be convenient if D cannot be enclosed tightly within a right parallelotope.
2. Conditioning to data. Suppose that the simulated random field has to be conditioned to a set of data scattered in space, a situation of interest in most geosciences applications. In such a case, the conditioning process requires performing the simulation at the (irregularly spaced) data locations [8, 20, 22].
3. Composition of random fields. Suppose that the simulated random field is of the form

   $$\forall \boldsymbol{x} \in \mathbb{R}^d, Z(\boldsymbol{x}) = Y_{\alpha,1}[T(\boldsymbol{x})],$$

   where $Y_{\alpha,1}$ is defined as in Eq. 3 (with $0<\alpha<2$) and T is a zero-order intrinsic random field with semi-variogram γ_T in $\mathbb{R}^d$. It is easy to show that Z is a zero-order intrinsic random field with a semi-variogram proportional to ${\gamma_T}^{\alpha/2}$ [40]. Simulating Z amounts to simulating T first, then $Y_{\alpha,1}$ at the locations in $\mathbb{R}$ defined by the realization of T, which have no reason to be regularly spaced.
4. Regularization. Suppose that one is interested in simulating a regularized random field

   $$\forall \boldsymbol{x} \in \mathbb{R}^d, Z(\boldsymbol{x}) = \int Y_{\alpha,d}(\boldsymbol{x}+\boldsymbol{h})\, p(\boldsymbol{h})\, d\boldsymbol{h},$$

   where $p(.)$ is a weighting function and $Y_{\alpha,d}$ is the random field defined in Eq. 21. One example of regularization has been seen in Eq. 24 for simulating a random measure with logarithmic generalized covariance, in which $p(.)$ was the indicator of a ball in $\mathbb{R}^d$. Other kinds of weighting functions could be considered, for instance, a d-variate normal density function that is the product of d marginal normal densities with mean 0 and standard deviation a. With the notations of Eq. 21, it comes

   $$Z(\boldsymbol{x}) = \theta_{\alpha,d}(R)\, \exp\left\{-\frac{(2\pi R a)^2}{2}\right\} \cos\left(2\pi R\, <\boldsymbol{x}, \boldsymbol{U}> + \phi\right).$$

   The regularization is performed by using the expression of $Y_{\alpha,d}$ as a cosine function, not by a weighted average of the values obtained over a fine grid.
5. Differentiation. Suppose that one is interested in simulating an intrinsic random field together with its partial derivatives, a problem of interest in geothermy, meteorology, and hydrogeology for characterizing heat, air, or water flows [14, 17, 21, 31, 34]. As for the regularization problem, the partial derivatives can be calculated directly from the functional expression of the intrinsic random field (Eqs. 21 to 23), with no need for a discretization over a regular grid.

Appendix

Consider a stationary random field Y defined in $\mathbb{R}^d$ with mean zero and unit variance. Let C be its covariance function and χ the associated spectral measure, such that [23, 29]:

$$\forall \boldsymbol{h} \in \mathbb{R}^d, C(\boldsymbol{h}) = \int_{\mathbb{R}^d} e^{i\langle \boldsymbol{\omega}, \boldsymbol{h}\rangle} \chi(d\boldsymbol{\omega}). \tag{30}$$

In particular, the integral of the spectral measure is the variance (also called *total power*) of the random field:

$$C(\boldsymbol{0}) = \int_{\mathbb{R}^d} \chi(d\boldsymbol{\omega}) = 1.$$

Assuming that χ has a probability density function f (a situation that occurs when C is absolutely integrable in $\mathbb{R}^d$), Eq. 30 becomes

$$\forall \boldsymbol{h} \in \mathbb{R}^d, C(\boldsymbol{h}) = \int_{\mathbb{R}^d} \cos\left(\langle \boldsymbol{\omega}, \boldsymbol{h}\rangle\right) f(\boldsymbol{\omega}) d\boldsymbol{\omega}. \tag{31}$$

A spectral turning bands approach to simulating Y consists in putting [32, 46]

$$\forall \boldsymbol{x} \in \mathbb{R}^d, Y(\boldsymbol{x}) = \sqrt{2}\, \cos(\langle \Omega, \boldsymbol{x}\rangle + \phi), \tag{32}$$

where ϕ is a random variable uniformly distributed on $[0,2\pi[$, whereas Ω is an independent random vector in $\mathbb{R}^d$ with probability density function f.

Let us now suppose that Ω has another probability density function in $\mathbb{R}^d$, say g, which is positive on the support of f. To compensate for the substitution of f by g, we shall replace Eq. 32 by the following expression:

$$\forall \boldsymbol{x} \in \mathbb{R}^d, Y(\boldsymbol{x}) = \sqrt{\frac{2f(\Omega)}{g(\Omega)}}\, \cos(\langle \Omega, \boldsymbol{x}\rangle + \phi). \tag{33}$$

For any $\boldsymbol{x}$ and $\boldsymbol{x}'$ in $\mathbb{R}^d$, the covariance between $Y(\boldsymbol{x})$ and $Y(\boldsymbol{x}')$ is

$$\begin{aligned}\operatorname{cov}\{Y(\boldsymbol{x}), Y(\boldsymbol{x}')\} &= 2E\left\{\frac{f(\Omega)}{g(\Omega)} \cos(\langle \Omega, \boldsymbol{x}\rangle + \phi)\, \cos(\langle \Omega, \boldsymbol{x}'\rangle + \phi)\right\} \\ &= \int_{\mathbb{R}^d} \frac{f(\omega)}{g(\omega)} \cos(\langle \omega, \boldsymbol{x} - \boldsymbol{x}'\rangle)\, g(\omega) d\omega \\ &= C(\boldsymbol{x} - \boldsymbol{x}'),\end{aligned}$$

the last equality being justified by Eq. 31. This implies that Y is second-order stationary with C as its covariance function. In

particular, suppose that f has a bounded support, say [−1,1], and let us choose for g a uniform probability density function on [−1,1]: This yields the spectral approaches proposed by Shinozuka and Jan [47] and Mantoglou and Wilson [37] for simulating stationary random fields.

As for intrinsic random fields, generalized covariances have spectral representations similar to Eq. 30 [8, 39]. However, unlike ordinary covariances, the integral of the spectral measure does not necessarily converge, as low frequencies may have an infinite power. To solve the simulation problem, Chilès [6] suggests defining a frequency threshold ω_0 such that cosine functions with frequencies less than ω_0 can be considered as constant at the scale of the domain where simulation is required. Hence, one can use Eq. 32, where the distribution of Ω is the spectral measure of the intrinsic random field conditioned by $|\Omega| > \omega_0$. Nonetheless, such a truncation of low frequencies introduces a bias in the reproduction of the generalized covariance. To avoid this drawback, the approach presented in this work relies on random fields of the form of Eq. 33 rather than Eq. 32. It can be viewed as an importance sampling technique that compensates for the under-sampling of low frequencies in the simulation process.

References

1. Ahrens, J.H., Dieter, U.: Generating gamma variates by a modified rejection technique. Commun. ACM **25**, (1), 47–54 (1982)
2. Besag, J., Mondal, D.: First-order intrinsic autoregressions and the de Wijs process. Biometrika **92**, (4), 909–920 (2005)
3. Box, G.E.P., Jenkins, G.M.: Time Series Analysis: Forecasting and Control. Holden-Day, San Francisco (1970)
4. Buttafuoco, G., Castrignano, A.: Study of the spatio-temporal variation of soil moisture under forest using intrinsic random functions of order k. Geoderma **128**, (3–4), 208–220 (2005)
5. Chauvet, P.: Processing data with a spatial support: Geostatistics and its methods. Cahiers de Géostatistique, Fascicule 4, 41 pp. Ecole des Mines de Paris, Fontainebleau (1993)
6. Chilès, J.P.: Quelques méthodes de simulation de fonctions aléatoires intrinsèques. In: de Fouquet, C. (ed.) Cahiers de Géostatistique, Fascicule 5, pp. 97–112. Ecole des Mines de Paris, Fontainebleau (1995)
7. Chilès, J.P., Allard, D.: Stochastic simulation of soil variations. In: Grunwald, S. (ed.) Environmental Soil-Landscape Modeling: Geographic Information Technologies and Pedometrics, pp. 289–321. CRC Press, Boca Raton (2005)
8. Chilès, J.P., Delfiner, P.: Geostatistics: Modeling Spatial Uncertainty. Wiley, New York (1999)
9. Chilès, J.P., Gable, R.: Three-dimensional modelling of a geothermal field. In: Verly, G., David, M., Journel, A.G., Maréchal, A. (eds.) Geostatistics for Natural Resources Characterization, pp. 587–598. Reidel, Dordrecht (1984)
10. Christakos, G., Thesing, G.A.: The intrinsic random field model in the study of sulfate deposition processes. Atmos. Environ., A–Gen. Topics **27**, (10), 1521–1540 (1993)
11. David, M.: Handbook of Applied Advanced Geostatistical Ore Reserve Estimation. Elsevier, Amsterdam (1988)
12. David, M., Crozel, D., Robb, J.M.: Automated mapping of the ocean floor using the theory of intrinsic random functions of order k. Mar. Geophys. Res. **8**, (1), 49–74 (1986)
13. Davis, M.W.: Production of conditional simulations via the LU triangular decomposition of the covariance matrix. Math. Geol. **19**, (2), 91–98 (1987)
14. de Fouquet, C.: Joint simulation of a random function and its derivatives. In: Kleingeld, W.J., Krige, D.G. (eds.) Geostats 2000 Cape Town, vol. 1. Geostatistical Association of Southern Africa, Cape Town (2001)
15. Delfiner, P., Chilès, J.P.: Conditional simulations: A new Monte-Carlo approach to probabilistic evaluation of hydrocarbon in place. SPE paper 6985, pp. 32 (1977)
16. Delhomme, J.P.: Spatial variability and uncertainty in groundwater flow parameters: a geostatistical approach. Water Resour. Res. **15**, (2), 269–280 (1979)
17. de Marsily, G.: Quantitative Hydrogeology: Groundwater Hydrology for Engineers. Academic, San Diego (1986)
18. Devroye, L.: Non-Uniform Random Variate Generation. Springer, New York (1986)
19. Dietrich, C.R., Newsam, G.N.: A fast and exact method for multidimensional Gaussian stochastic simulations. Water Resour. Res. **29**, (8), 2861–2869 (1993)
20. Dimitrakopoulos, R.: Conditional simulation of intrinsic random functions of order k. Math. Geol. **22**, (3), 361–380 (1990)
21. Dong, A.: Estimation géostatistique des phénomènes régis par des équations aux dérivées partielles. Doctoral thesis, Ecole des Mines de Paris, Paris (1990)
22. Emery, X., Lantuéjoul, C.: TBSIM: a computer program for conditional simulation of three-dimensional Gaussian random fields via the turning bands method. Comput. Geosci. **32**, (10), 1615–1628 (2006)
23. Feller, W.: An Introduction to Probability Theory and Its Applications, vol. 2, 2nd edn. Wiley, New York (1971)
24. Flandrin, P.: Wavelet analysis and synthesis of fractional Brownian motion. IEEE Trans. Inf. Theory **38**, (2), 910–917 (1992)
25. Fournier, A., Fussell, D., Carpenter, R.L.: Computer rendering of stochastic models. Commun. ACM **25**, (6), 371–384 (1982)
26. Gneiting, T., Sasvári, Z., Schlather, M.: Analogies and correspondences between variograms and covariance functions. Adv. Appl. Probab. **33**, (3), 617–630 (2001)
27. Gradshtein, I.S., Ryzhik, I.M.: Table of Integrals, Series and Products, 4th edn. Academic, New York (1965)
28. Journel, A.G.: Geostatistics for conditional simulation of ore-bodies. Econ. Geol. **69**, (5), 673–687 (1974)
29. Khinchin, A.Y.: Korrelationstheorie der stationären stochastischen Prozesse. Math. Ann. **109**, (1), 604–615 (1934)
30. Kitanidis, P.K.: Statistical estimation of polynomial generalized covariance functions and hydrologic applications. Water Resour. Res. **19**, (4), 909–921 (1983)
31. Kitanidis, P.K.: Generalized covariance functions associated with the Laplace equation and their use in interpolation and inverse problems. Water Resour. Res. **35**, (5), 1361–1367 (1999)
32. Lantuéjoul, C.: Non conditional simulation of stationary isotropic multigaussian random functions. In: Armstrong, M., Dowd, P.A. (eds.) Geostatistical Simulations, pp. 147–177. Kluwer, Dordrecht (1994)
33. Lantuéjoul, C.: Geostatistical Simulation: Models and Algorithms. Springer, Berlin (2002)
34. Le Cointe, P.: Kriging with partial differential equations in hydrogeology. Master's thesis, Université Pierre et Marie Curie, Ecole des Mines de Paris & Ecole Nationale du Génie Rural des Eaux et Forêts, Paris (2006)
35. Mandelbrot, B.B., Van Ness, W.J.: Fractional Brownian motions, fractional noises and applications. SIAM Rev. **10**, (4), 422–437 (1968)
36. Mantoglou, A.: Digital simulation of multivariate two- and three-dimensional stochastic processes with a spectral turning bands method. Math. Geol. **19**, (2), 129–149 (1987)

37. Mantoglou, A., Wilson, J.L.: The turning bands method for simulation of random fields using line generation by a spectral method. Water Resour. Res. **18**, (5), 1379–1394 (1982)
38. Matheron, G.: The Theory of Regionalized Variables and its Applications. Ecole des Mines de Paris, Paris (1971)
39. Matheron, G.: The intrinsic random functions and their applications. Adv. Appl. Probab. **5**, 439–468 (1973)
40. Matheron, G.: The internal consistency of models in geostatistics. In: Armstrong, M. (ed.) Geostatistics, vol. 1, pp. 21–38. Kluwer, Dordrecht (1989)
41. Pardo-Igúzquiza, E., Dowd, P.A.: IRFK2D: a computer program for simulating intrinsic random functions of order k. Comput. Geosci. **29**, (6), 753–759 (2003)
42. Saupe, D.: Algorithms for random fractals. In: Peitgen, H.O., Saupe, D. (eds.) The Science of Fractal Images, pp. 71–113. Springer, New York (1988)
43. Schlather, M.: An Introduction to Positive Definite Functions and to Unconditional Simulation of Random Fields. Technical Report ST-99–10, Lancaster University (1999)
44. Sellan, F.: Wavelet transform based fractional Brownian-motion synthesis. Compte Rendu de l'Académie des Sciences, Série I Mathématique **321**, (3), 351–358 (1995)
45. Shiganov, I.S.: Refinement of the upper bound of the constant in the central limit theorem. J. Math. Sci. **35**, (3), 2545–2550 (1986)
46. Shinozuka, M.: Simulation of multivariate and multidimensional random processes. J. Acoust. Soc. Am. **49**, (1), 357–367 (1971)
47. Shinozuka, M., Jan, C.M.: Digital simulation of random processes and its applications. J. Sound Vib. **25**, (1), 111–128 (1972)
48. Stein, M.L.: Local stationarity and simulation of self-affine intrinsic random functions. IEEE Trans. Inf. Theory **47**, (4), 1385–1390 (2001)
49. Stein, M.L.: Fast and exact simulation of fractional Brownian surfaces. J. Comput. Graph. Stat. **11**, (3), 587–599 (2002)
50. Suárez Arriaga, M.C., Samaniego, F.: Intrinsic random functions of high order and their application to the modeling of non-stationary geothermal parameters. In: Proceedings of the Twenty-third Workshop on Geothermal Reservoir Engineering, pp. 169–175. Technical report SGP-TR-158, Stanford University, Stanford (1998)
51. Tompson, A.F.B., Ababou, R., Gelhar, L.W.: Implementation of the three-dimensional turning bands random field generator. Water Resour. Res. **25**, (8), 2227–2243 (1989)
52. Voss, R.F.: Random fractal forgeries. In: Earnshaw, R.A. (ed.) Fundamental Algorithms for Computer Graphics, pp. 805–835. Springer, Berlin (1985))
53. Yin, Z.M.: New methods for simulation of fractional Brownian motion. J. Comput. Phys. **127**, (1), 66–72 (1996)
54. Zeldin, B.A., Spanos, P.D.: Random field representation and synthesis using wavelet bases. J. Appl. Mech.—Trans ASME **63**, (4), 946–952 (1996)